Biomaterials 143 (2017) 149–158

Contents lists available at ScienceDirect

Biomaterials

journal homepage: www.elsevier.com/locate/biomaterials

PNIPAAm-co-Jeffamine® (PNJ) scaffolds as *in vitro* models for niche enrichment of glioblastoma stem-like cells

John M. Heffernan [a, b], James B. McNamara [a, c], Sabine Borwege [a], Brent L. Vernon [b], Nader Sanai [a], Shwetal Mehta [a], Rachael W. Sirianni [a, b, *]

[a] Barrow Brain Tumor Research Center, Barrow Neurological Institute, 350 W Thomas Ave, Phoenix, AZ, 85013, USA
[b] School of Biological and Health Systems Engineering, Arizona State University, PO Box 879709, Tempe, AZ, 85287, USA
[c] Department of Chemistry and Biochemistry, University of Arizona, 1306 E. University Blvd., Tucson, AZ, 85721, USA

ARTICLE INFO

Article history:
Received 16 February 2017
Received in revised form
28 April 2017
Accepted 3 May 2017
Available online 6 May 2017

Keywords:
Brain tumor initiating cells
Cancer stem cells
Radioresistance
Tissue engineering
Temperature responsive polymer scaffolds

ABSTRACT

Glioblastoma (GBM) is the most common adult primary brain tumor, and the 5-year survival rate is less than 5%. GBM malignancy is driven in part by a population of GBM stem-like cells (GSCs) that exhibit indefinite self-renewal capacity, multipotent differentiation, expression of neural stem cell markers, and resistance to conventional treatments. GSCs are enriched in specialized niche microenvironments that regulate stem phenotypes and support GSC radioresistance. Therefore, identifying GSC-niche interactions that regulate stem phenotypes may present a unique target for disrupting the maintenance and persistence of this treatment resistant population. In this work, we engineered 3D scaffolds from temperature responsive poly(N-isopropylacrylamide-co-Jeffamine M-1000® acrylamide), or PNJ copolymers, as a platform for enriching stem-specific phenotypes in two molecularly distinct human patient-derived GSC cell lines. Notably, we observed that, compared to conventional neurosphere cultures, PNJ cultured GSCs maintained multipotency and exhibited enhanced self-renewal capacity. Concurrent increases in expression of proteins known to regulate self-renewal, invasion, and stem maintenance in GSCs (NESTIN, EGFR, CD44) suggest that PNJ scaffolds effectively enrich the GSC population. We further observed that PNJ cultured GSCs exhibited increased resistance to radiation treatment compared to GSCs cultured in standard neurosphere conditions. GSC radioresistance is supported *in vivo* by niche microenvironments, and this remains a significant barrier to effectively treating these highly tumorigenic cells. Taken in sum, these data indicate that the microenvironment created by synthetic PNJ scaffolds models niche enrichment of GSCs in patient-derived GBM cell lines, and presents tissue engineering opportunities for studying clinically important behaviors such as radioresistance *in vitro*.

1. Introduction

Glioblastoma (GBM), the most common primary brain tumor in adults, has a devastatingly low 4.7% 5-year survival rate with a median survival of only 15 months [1,2]. Standard treatments, including surgical tumor resection, radiation, and chemotherapy, provide little long-term benefit, and relapse is nearly universal. GBMs are heterogeneous tumors composed of neoplastic cells that exhibit a hierarchy of tumorigenic potential. In accordance with the cancer stem cell hypothesis, this hierarchy is directed by a small population of cells that exhibit the greatest capacity for tumor formation [3]. These GBM stem-like cells (GSCs) display many similarities to normal adult neural stem cells (NSCs), including a capacity for indefinite self-renewal, multipotent differentiation, and expression of NSC marker proteins [4–7]. GSCs are also highly tumorigenic [8], invasive [9], and resistant to both radiation [10] and chemotherapy [11,12]. GSCs that evade and survive treatment are hypothesized to play a prominent role in tumor recurrence [3].

In vivo, GSCs are concentrated in specialized niches that regulate stem phenotypes [13,14]. In the absence of essential niche regulation *in vitro*, GSCs can be maintained and propagated in NSC culture conditions as multicellular neurospheres [15]. However, neurosphere cultures can hinder effective enrichment of GSCs.

* Corresponding author. Barrow Neurological Institute Neural Research Center, Room 436, 350 W. Thomas Road, Phoenix, AZ, 85013, USA.
E-mail address: rachael.sirianni@dignityhealth.org (R.W. Sirianni).

http://dx.doi.org/10.1016/j.biomaterials.2017.05.007
0142-9612/

Diffusion of nutrients and signaling factors that are essential for stem maintenance is limited by the size and number of cells within multicellular neurospheres [16]. The resulting intra-sphere nutrient gradients lead to growth of a poorly controlled population of stem, non-stem, apoptotic, and necrotic cells [17–19]. GSCs are commonly enriched and purified from these cultures by fluorescence activated cell sorting (FACS) for cell-surface biomarkers (including CD133 [7,8], SSEA-1/CD15 [20], Integrin α6 [21]), which is typically paired with functional analysis of stem cell behaviors [22]. However, the use of cell-surface markers alone contributes to high false positive rates of GSC identification [23]. Therefore, it is essential to analyze GSC populations at the functional level, to identify stem cell behaviors such as multipotency and self-renewal.

Although neurosphere culture conditions provide a pseudo three-dimensional (3D) context for cell growth, this format presents limited opportunity for controlling and studying microenvironmental influences on stem cell behavior. Microenvironmental regulation of stem-specific behaviors has been investigated extensively in regenerative medicine by utilizing 3D biomaterials, but comparably few examples exist in GSC research. Acquisition of selected stem characteristics has been reported for U87 and U251 GBM cell lines cultured in 3D scaffolds [24–27]. However, serum cultured long-term established GBM cell lines like U87 and U251 do not maintain the functional stem characteristics of primary GSCs, nor do they provide an accurate representation of GBM biology [4,5,15,28]. This severely limits the relevance of using immortalized cells to study either GBM or GSC biology. Recently, Li et al. reported that multipotent patient-derived GBM cells could be maintained in Mebiol® Gel (Cosmo Bio USA), a temperature responsive poly(N-isopropylacrylamide) (PNIPAAm) based hydrogel scaffold [29]. In addition, Hubert et al. described the development of large heterogeneous GBM organoids from patient-derived GSCs cultured in Matrigel® [30]. These prior works emphasize the significance of using biomaterials to study GSCs, but 3D culture conditions that actively enrich the full complement of GSC functional phenotypes (e.g., multipotency, self-renewal, treatment resistance) have not been defined *in vitro*.

In this study, we engineered poly(N-isopropylacrylamide-co-Jeffamine® M - 1000 acrylamide) (PNJ) copolymers as tunable scaffolds for 3D GSC culture. PNJ copolymers exhibit a lower critical solution temperature (LCST) phase transition when heated in aqueous solution [31–33]. As a result, these materials encapsulate cells in physically crosslinked viscoelastic scaffolds at body temperature and easily release the cells by cooling to room temperature. We have previously reported the utility of this platform for enabling serial expansion of immortalized GBM cell lines in 3D [33]. Here, we describe conditions under which two patient-derived GBM lines are cultured in PNJ scaffolds to actively enrich GSC phenotypes, as measured by the full diversity of stem cell behaviors expected to drive tumor malignancy; this analysis includes multipotency, self-renewal capacity, expression of stem cell markers, and radiation resistance. For the purpose of these studies, we focus on self-renewal capacity, as measured by the *in vitro* limiting dilution assay, as the most direct approach for evaluation of relative GSC fractions under distinct culture conditions. We postulate that PNJ scaffolds may function similar to the native niche by serving as a depot for growth factors that maintain the GSC population [14]. The broader significance of these findings is that radioresistance, which is hallmark feature of GSC biology, is supported *in vivo* by microenvironmental factors that may be deficient or completely absent from standard cultures. Therefore, by defining microenvironmental mechanisms that drive GSC enrichment and radioresistance, 3D PNJ cultures may improve the accuracy and understanding of GSC responses to radiation *in vitro*.

2. Methods

2.1. Materials

All chemicals were reagent grade and purchased from Sigma Aldrich (St. Louis, MO, USA) unless otherwise stated. All cell culture reagents were purchased from Thermo Fisher Scientific (Waltham, MA, USA) unless otherwise stated. N-isopropylacrylamide (NIPAAm) purchased from Tokyo Chemical Company (Portland, OR, USA) was purified by recrystallization from hexane. 2,2′-Azobisisobutyronitrile (AIBN) was purified by recrystallization from methanol. Jeffamine® M-1000 was generously donated by the Huntsman Corporation (Salt Lake City, UT, USA). Jeffamine® M-1000 acrylamide (JAAm) was synthesized as previously reported [31,32].

2.2. Polymer synthesis

Poly(N-isopropylacrylamide-co-Jeffamine® M-1000 acrylamide) or PNJ copolymers were synthesized as previously described [32,33]. Briefly, radical polymerization of NIPAAm and JAAm monomers was initiated with AIBN (7 mmol AIBN/mol monomer) in anhydrous benzene. Copolymer feed ratios of NIPAAm:JAAm by mass were 90:10 (PNJ10), 85:15 (PNJ15), or 80:20 (PNJ20). All PNJ copolymers were purified by dialysis (3500 MWCO) against diH_2O at 4 °C and sterilized with ethylene oxide. Chemical compositions were analyzed by ^1H NMR in D_2O (400 MHz Varian Inova, Agilent Technologies, Santa Clara, CA, USA).

2.3. Rheology

The mechanical properties of PNJ scaffolds were measured at various concentrations by rheology. PNJ solutions were prepared at 5, 7.5, and 10 wt% in PBS at room temperature and placed on a parallel plate rheometer with a temperature controlled stage (MCR-101, Anton Paar, Ashland, VA, USA). Samples were rapidly heated to 37 °C and subjected to a frequency sweep (0.1–10 Hz) with 0.5% shear strain deformation and normal force control (50 mN) to determine the storage (G′) and loss (G″) modulus.

2.4. Patient-derived primary GSC culture

Patient tissue samples were acquired from the Biobank Core Facility at St. Joseph's Hospital and Medical Center and Barrow Neurological Institute (BNI) (Phoenix, AZ, USA). All samples were collected and transmitted according to the Biobank Institutional Review Board's approved protocol. In our previous work, two patient-derived GSC cell lines, GB3 [35,36] and GB7 [35], were established from primary GBM tumors surgically resected at BNI and characterized as human GSC models. GB3, classified as a proneural GBM subtype, was characterized through *in vitro* testing of stem behaviors, and *in vivo* via orthotopic transplantation. GB7 was classified as a classical GBM subtype through *in vitro* characterization of stem behaviors. GSCs were propagated in cell culture as non-adherent neurospheres grown in GSC media (DMEM/F12 media supplemented with B27, N2 and penicillin/streptomycin) in low-attachment poly(hydroxyethylmethacrylate) (polyHEMA) coated plates. Cultures were supplemented with 20 ng/mL of epidermal growth factor (EGF) and basic fibroblast growth factor (bFGF) (Merk Millipore, Billerica, MA, USA) every 2–3 days.

2.5. GSC culture in PNJ scaffolds

PNJ copolymers were dissolved at 5 wt% in GSC media overnight

at 4 °C. GSCs were dissociated with Accutase to a single cell suspension, counted (Cellometer Mini, Nexcelom, Lawrence, MA, USA), and resuspended in PNJ-media solution at room temperature (350k cells/mL). Cultures were then incubated at 37 °C to crosslink PNJ scaffolds and encapsulate cells in 3D culture. After 48 h, an equal volume of warm culture media was added above the scaffold. Every 2–3 days, scaffolds were supplemented with EGF and FGF (20 ng/mL) after being solubilized at room temperature to allow for distribution of nutrients. Upon warming the cultures back to 37 °C, the scaffolds were reformed and encapsulated the freshly added growth factors. At confluence (7–14 days for GB7; 14–21 days for GB3), PNJ scaffolds were cooled to room temperature, diluted in PBS, and centrifuged to recover live cells. In all experiments, PNJ cultures were compared with neurosphere cultures described in section 2.4.

2.6. Analysis of neurosphere area

GSCs cultured in PNJ scaffolds and in standard neurosphere conditions were imaged using brightfield microscopy (Zeiss Axio Observer A1) over the duration of the culture period. The area of GSC spheres ($n > 225$ spheres per condition per day) was measured using ImageJ (NIH) and compared across culture conditions.

2.7. GSC multipotent differentiation

GSC spheres were dissociated with Accutase to a single cell suspension. Cells were differentiated by culturing GSCs in serum supplemented media (DMEM + 10% FBS + 1% penicillin/streptomycin) on glass coverslips coated with poly-*d*-lysine. Media was replaced every 2–3 days for 14 days, after which cells were immunostained for markers of differentiation into astrocytes (GFAP), oligodendrocytes (GALC), and neurons (TUBULIN βIII). Cells were fixed with 4% PFA for 10 min, permeabilized and blocked for 30–60 min in PBST + 5% goat serum, and incubated in primary antibodies (Table 1) diluted in blocking buffer at 4 °C overnight. Cells were stained with fluorescent secondary antibodies (Table 1) diluted in blocking buffer at 37 °C for 30 min, counterstained with DAPI (3 ng/mL) for 10 min, and mounted on slides prior to imaging with an inverted fluorescence confocal microscope (Zeiss LSM 710 Axio Observer Z1).

2.8. Limiting dilution assay

GSCs were dissociated with Accutase and cultured at low initial densities (1–50 cells) in polyHEMA coated 96-well plates. After 7 days, wells were imaged with brightfield microscopy (Zeiss Axio Observer A1) to determine sphere formation at each initial density. Wells negative for sphere formation (% nonresponsive) were counted. This experiment was replicated 4 times with at least $n = 12$ samples for each initial cell density.

2.9. Western blot analysis

To prepare protein lysates, GSCs were lysed in ice cold RIPA buffer supplemented with fresh protease and phosphatase inhibitors. Protein concentration was measured using a standard Bradford assay. Western blots were run with 40 μg samples separated by gel electrophoresis on a 10% bisacrylamide gel (Bio-Rad, Hercules, CA, USA). Proteins were transferred to a polyvinylidene difluoride (PVDF) membrane at 4 °C (Bio-Rad, USA). Membranes were blocked in 5% milk TBST and incubated with primary antibodies (Table 1) diluted in blocking solution shaking overnight at 4 °C. Membranes were then incubated with fluorescent secondary antibodies (Table 1) diluted in blocking solution at room temperature. Blots were analyzed using a fluorescence reader (LiCor Odyssey CLx). Protein expression data is represented as the mean of $n = 4$ independent experiments.

2.10. Radiation sensitivity

GSCs were irradiated (RAD Source 2000, RAD Source) in PNJ scaffolds or in neurosphere conditions with 2 or 10 Gy ionizing radiation. Immediately following treatment, cells were recovered from cultures, counted, and re-plated as single cells at equivalent densities in neurosphere growth conditions. Cell viability was measured with Cell Titer Glo (Promega) in comparison to a matched non-treated control 48 h after radiation.

2.11. Statistical testing

Statistical tests for neurosphere size data (Section 2.6) were performed in Prism 5 (GraphPad) using a one-way ANOVA test with Bonferroni post-test. Statistical testing for limiting dilution data (Section 2.8) was performed using a chi-squared test through the extreme limiting dilution analysis (ELDA) software previously published by Hu and Smyth [37]. Statistical significance is reported for $p < 0.05$.

Table 1
Primary and secondary antibodies used in this study.

	Company	Product #	Host	Dilution	Application
Primary Antibodies					
NESTIN	Novus Biologicals	NB300-266	Mouse	1:2000	WB
EGFR	Abcam	AB52894	Rabbit	1:10000	WB
CD44	Cell Signaling Technologies	3570S	Mouse	1:2000	WB
SOX2	Cell Signaling Technologies	3579S	Rabbit	1:2000	WB
OLIG2	[34]	DF308	Rabbit	1:1000	WB
PDGFRα	Santa Cruz	SC-338	Rabbit	1:1000	WB
VINCULIN	Abcam	SPM227	Mouse	1:10000	WB
GFAP	Merck Millipore	AB9598	Rabbit	1:200	IF
GALC	Merck Millipore	MAB342	Mouse	1:250	IF
TUBULIN βIII	Merck Millipore	MAB1637	Mouse	1:200	IF
Secondary Antibodies					
Alexa Fluor 488	Thermo Fisher	A21121	Goat anti-Mouse IgG1	1:1000	IF
Alexa Fluor 488	Thermo Fisher	A21151	Goat anti-Mouse IgG3	1:1000	IF
Alexa Fluor 488 and 568	Thermo Fisher	A11008/A11011	Goat anti-Rabbit IgG	1:1000	IF
DyLight 680	Thermo Fisher	PI35519	Goat anti-Mouse IgG	1:10000	WB
DyLight 800	Thermo Fisher	PISA510036	Goat anti-Rabbit IgG	1:10000	WB

3. Results

3.1. PNJ scaffolds

Three formulations of PNJ copolymers (Fig. 1A) were synthesized by varying the concentration of JAAm (10%, 15%, and 20%) during polymerization with NIPAAm. JAAm incorporation was measured by ^{1}H NMR and the resulting formulations are distinguished by their JAAm content: PNJ10, PNJ15, and PNJ20 (Table 2). Similar to our previous reports, the LCST for each copolymer was measured by rheology between 29 and 31 °C (data not shown). This characteristic allows for PNJ copolymer solutions to remain soluble when handled at room temperature (~25 °C) and to form physically crosslinked scaffolds when heated to body temperature (~37 °C) [31–33]. We observed that the three PNJ formulations formed viscoelastic scaffolds with storage and loss moduli that decreased in response to decreasing total polymer concentration (Fig. 1B). JAAm incorporation also affected scaffold stiffness; for 7.5 wt% and 5 wt%, higher JAAm content produced less stiff gels, whereas we observed that PNJ15 scaffolds exhibited increased stiffness compared to PNJ10 scaffolds when formed at 10 wt%. This observation, although unexpected, was repeatable across independent polymer batches. We also observed that the PNJ10 scaffolds were slower to dissolve when formed at 10 wt% than the PNJ15 and PNJ20 scaffolds; it is thus possible that, at 10 wt%, a higher concentration of polymer facilitated additional hydrophobic interactions to promote phase separation, thus generating mild syneresis and a plateau in the PNJ10 modulus. Taken in sum, these data demonstrate the ability to produce a library of PNJ materials with scaffold stiffness (i.e., G′) tunable between 153 and 1240 Pa.

3.2. GSCs in PNJ scaffolds

Patient-derived primary GSCs (GB3 and GB7) were cultured in soft 5 wt% PNJ scaffolds, which possess brain-mimetic stiffness (153 Pa - 325 Pa). We compared the growth of GSCs in these conditions to standard neurosphere culture conditions as a control. In neurosphere culture, GSCs displayed as expected, high variability in sphere sizes. Conversely, we observed that GSCs cultured in 3D grew as individual spheres that remained smaller and more uniform in size due to decreased cell-cell contact within the scaffold (Fig. 2A). These qualitative observations were quantified by measuring the area of neurospheres in both neurosphere and 3D culture (Fig. 2B). Both GB3 and GB7 grew as significantly smaller spheres with a higher degree of uniformity in 3D compared to controls. These data indicate that PNJ scaffolds segregate cells to prevent sphere aggregation, a key drawback of neurosphere culture.

Table 2
Properties of PNJ copolymers. Monomer incorporation (NIPAAm wt% (x): JAAm wt% (y)) was measured by ^{1}H NMR in D_2O. The weight average molecular weight (M_w) and polydispersity (P_D) were determined by GPC with THF as the mobile phase.

Polymer	NIPAAm wt% (x):JAAm wt % (y)		Molecular Weight	
	Feed	Composition	M_W ($\times 10^6$ Da)	P_D
PNJ10	90:10	92.4:7.6	1.671	1.047
PNJ15	85:15	89.3:10.7	1.649	1.133
PNJ20	80:20	85.2:14.8	1.182	1.076

3.3. GSC multipotency and self-renewal

Live GSCs were recovered from PNJ scaffolds by cooling the cultures to room temperature to induce scaffold phase transition [33]. The multipotency of the recovered cells was determined by differentiating GSCs in serum supplemented media. After two weeks, the differentiated cells were stained for markers of neuronal lineage (βIII-tubulin), oligodendrocyte lineage (GalC), and astrocytic lineage (GFAP). GB3 and GB7 cells grown in all PNJ and control cultures were observed to differentiate into each of the assayed neural subtypes (Fig. 3) indicating that multipotency was maintained in control and PNJ culture conditions.

We also measured the self-renewal capacity of the recovered cells in an *in vitro* limiting dilution assay (Fig. 4). Given the initial cell density and resulting probability of neurosphere formation, we determined the concentration of clonal cells in populations taken from each culture condition using extreme limiting dilution analysis [37]. The stem cell frequency of GB3 cells cultured in neurosphere conditions was 1 in 6.7 (95% CI: [5.68, 7.97]) compared to 1 in 4.3 (95% CI: [3.68, 7.97]), 4.0 (95% CI: [3.39, 4.63]), and 3.8 (95% CI: [2.05, 4.03]) for PNJ10, PNJ15, and PNJ20 respectively. For GB7 cells, the stem cell frequency in neurosphere conditions was 1 in 14.0 (95% CI: [11.41, 17.22]) compared to 1 in 6.9 (95% CI: [5.72, 8.45]), 8.0 (95% CI: [6.57, 9.75]), and 6.4 (95% CI: [5.29, 7.80]) for PNJ10, PNJ15, and PNJ20 respectively. For both GB3 and GB7, all three PNJ scaffold formulations resulted in a significant ($p < 0.01$)

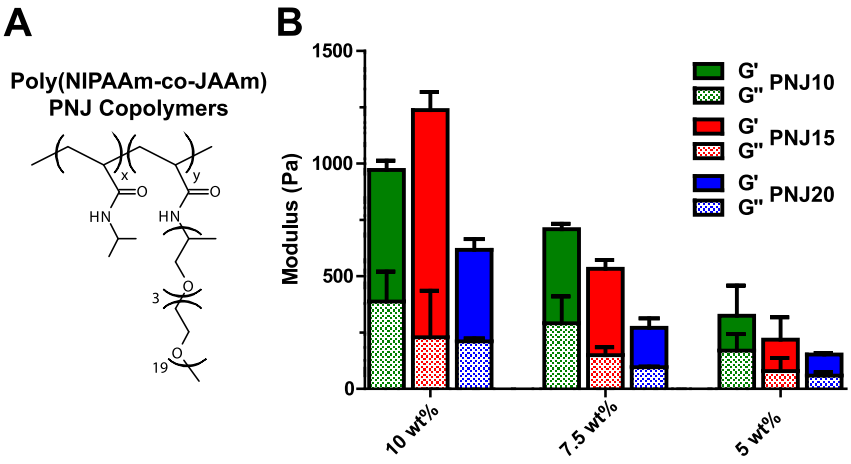

Fig. 1. (A) Chemical structure of PNJ copolymers. (B) Complex modulus of PNJ scaffolds formed at 10 wt%, 7.5 wt% and 5 wt% measured by rheology. Rheological measurements (n = 2) were made with samples heated to 37 °C.

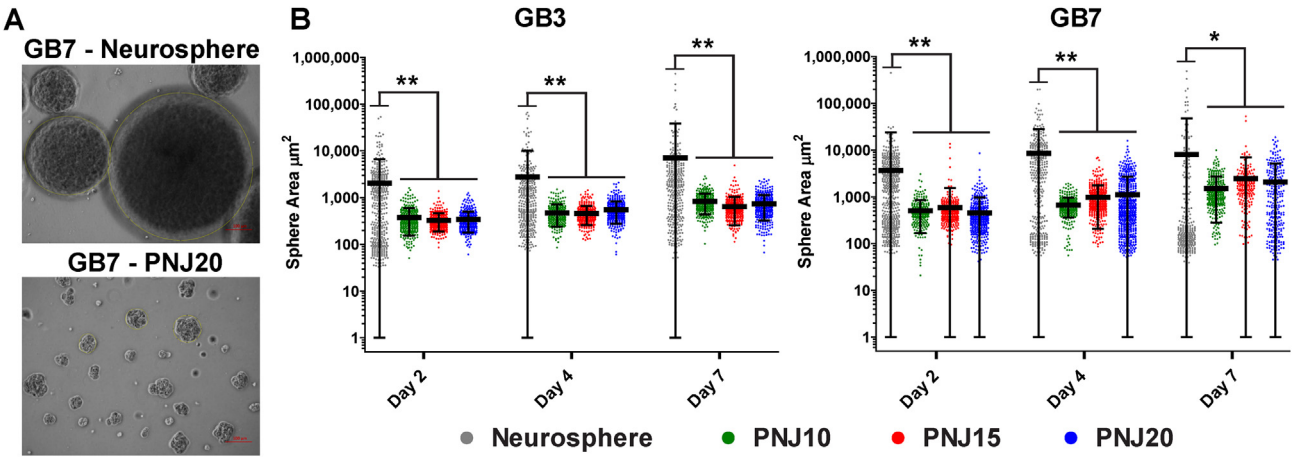

Fig. 2. (A) Brightfield images of GB7 spheres in neurosphere conditions and PNJ20 scaffolds after 7 days of culture. (B) Quantification of 2D GSC sphere area during culture in neurosphere or PNJ scaffold conditions. Spheres were significantly smaller in all PNJ scaffolds at all time points compared to neurosphere cultures (*$p < 0.05$ and **$p < 0.01$; 1-way ANOVA with Tukey post-test; $n > 225$ for each data set).

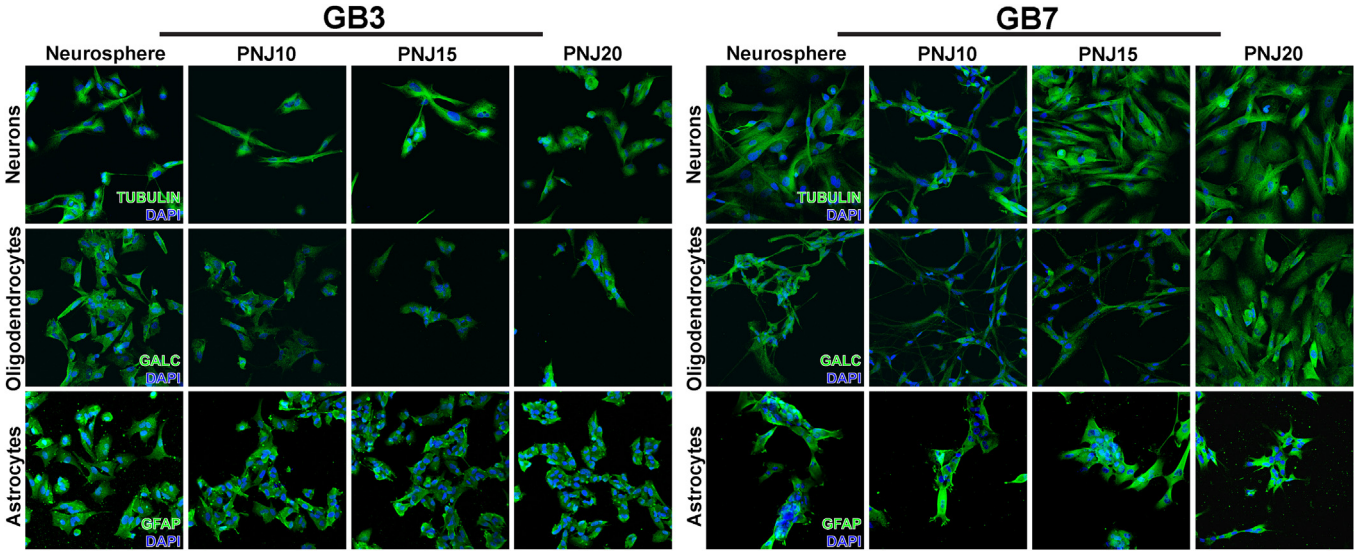

Fig. 3. Multipotency of GB7 and GB3 GSCs measured by immunofluorescence staining for differentiation markers (green) along with DAPI nuclei counterstaining (blue). Cells cultured in both neurosphere and PNJ scaffold conditions were capable of differentiating into neuronal (Tubulin), oligodendrocyte (GalC), and astrocytic (GFAP) lineages (nonlinear adjustments were made to some images for visual clarity). (For interpretation of the references to colour in this figure legend, the reader is referred to the web version of this article.)

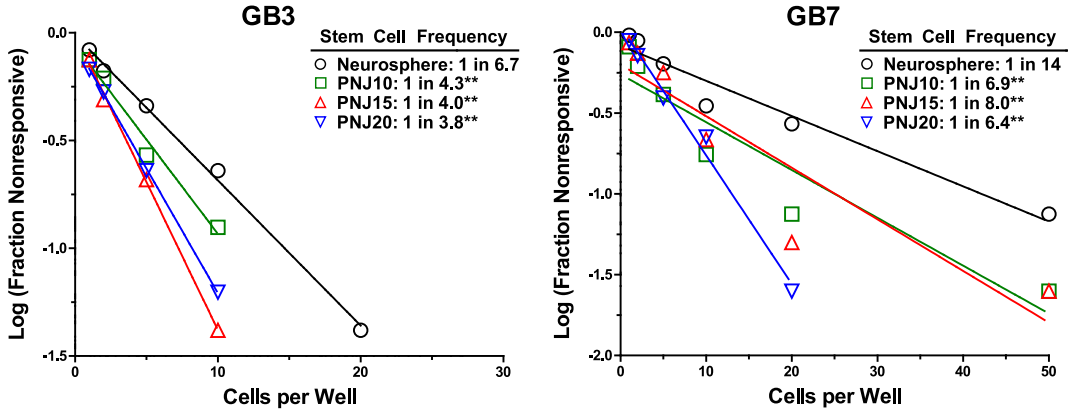

Fig. 4. Self-renewal and stem cell frequency of GB7 and GB3 cells measured in a limiting dilution assay. Stem cell frequency was significantly increased in all PNJ cultures compared to control (**$p < 0.01$; chi-squared test for pairwise differences).

increase in stem cell frequency compared to neurosphere culture; GSC enrichment in scaffolds was highest for the GB7 cell line.

3.4. Stem marker expression in PNJ scaffolds

For comprehensive characterization of the GSC phenotype, we measured the expression of proteins important to both GBM and GSC biology in PNJ cultured cells. In these assays, we measured expression of NESTIN along with the transcription factors SOX2 and OLIG2 as markers of GBM stemness [23]. We also measured expression of the receptor tyrosine kinases (RTKs) for epidermal growth factor (EGFR) and platelet derived growth factor alpha (PDGFRα) along with the hyaluronic acid receptor CD44, all of which are associated with malignant GBM phenotypes, GSC maintenance, and interactions with the GSC niche [23,38,39]. In both cell lines, we observed an increase in NESTIN and EGFR expression in all scaffold conditions compared to neurosphere controls (Fig. 5). CD44 expression was also increased in PNJ cultured GB3 cells compared to neurosphere controls. In GB7, CD44 was increased in PNJ10 and PNJ20 scaffolds but not in PNJ15. All other proteins tested did not display notable differences between scaffold and control cultures. The increases in expression of these proteins provides further evidence of GSC maintenance and enrichment in PNJ scaffolds.

3.5. Radiation sensitivity in PNJ scaffolds

Radiation resistance is a hallmark feature of GSCs *in vivo* and is actively supported by the GSC niche microenvironment. Here, we compared the viability of neurosphere and PNJ cultured GSCs following radiation treatment at a clinically relevant dose (2 Gy) and a high dose (10 Gy). Both GB3 and GB7 cells displayed a dose response to treatment in neurosphere conditions with GB3 cells exhibiting a more resistant baseline phenotype. Interestingly, 3D culture in PNJ scaffolds, regardless of composition, significantly increased resistant behavior in both GB3 and GB7 cells at both levels of treatment (Fig. 6). This provides further evidence for the positive regulatory effect that the 3D PNJ microenvironment exerts on GSCs in culture.

4. Discussion

GSCs are distinguished within the broader population of GBM tumor cells by their multipotency, self-renewal capacity, NSC marker expression, and radioresistance [4–7]. Together, these phenotypic features lead GSCs to be highly tumorigenic and likely drivers of tumor recurrence following conventional treatments such as radiation therapy. GSCs, similar to NSCs, are enriched in distinct niche microenvironments comprised of both cellular (e.g. immune cells) and non-cellular (e.g. extracellular matrix) components that provide critical regulatory signaling cues. In addition, niche inputs are also implicated in actively supporting treatment resistance in these cells [13,14,40–42]. Therefore, identifying mechanisms of GSC regulation contributed by the physical microenvironment may lead to options for targeting the niche with therapeutics that disrupt their regulatory capacity and sensitize otherwise resistant cells to treatment.

The complexity and anisotropy of the GSC microenvironments

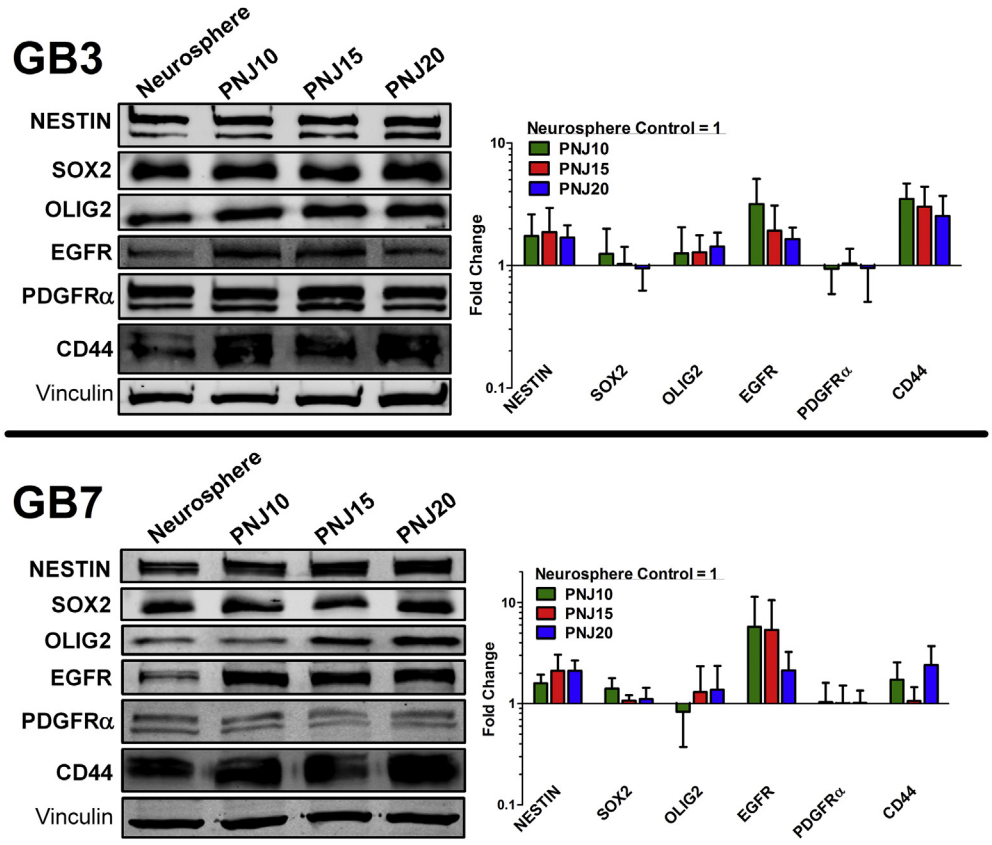

Fig. 5. Expression of GSC marker proteins in PNJ scaffolds compared to neurosphere control cultures measured by western blot. In GB3 (n = 4), NESTIN, EGFR, and CD44 expression were increased in PNJ scaffolds compared to controls. In GB7 (n = 4), expression of NESTIN and EGFR were again increased in all scaffold conditions, while CD44 was increased in PNJ10 and PNJ20 scaffolds. Nonlinear adjustments were made to some images for visual clarity.

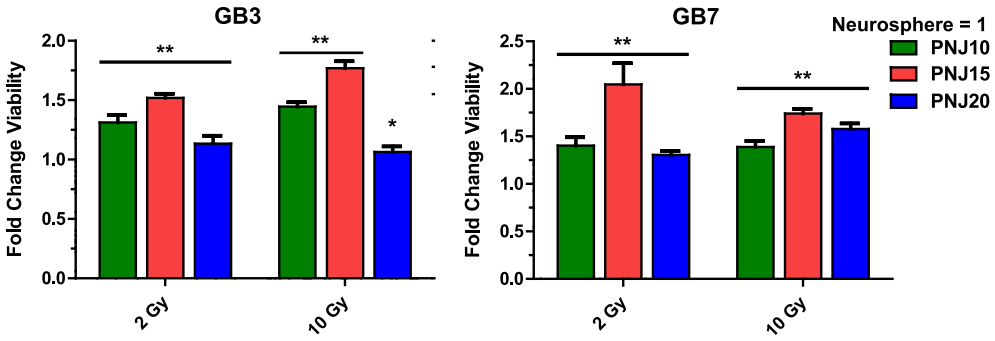

Fig. 6. Viability of PNJ cultured GSCs following low dose (2 Gy) and high dose (10 Gy) radiation is significantly higher compared to neurosphere cultures (fold change calculated in comparison to neurosphere controls; mean values are reported with SD; n = 12 replicates; *p < 0.05 and **p < 0.01; 2-way ANOVA with Bonferonni post-test).

complicates analyzing specific regulatory contributions *in vivo*. As a result, three-dimensional scaffolds have been routinely used to measure various interactions between GBM cell lines or GSCs and their local microenvironment by us [33,43] and others [24,29,30,44–52]. Although immortalized cell lines are proven tools in GBM research, they are poor biological models of the clinical condition and do not maintain functional GSCs [4,5,15,28]. In addition, 3D culture conditions that enrich GSCs, as measured by their functional phenotype, and concurrently support radioresistance have not been reported. Thus, there remains a significant need to engineer physical microenvironments to study GSC-niche interactions and their contribution to therapeutic response. Here, we designed a synthetic polymeric biomaterial platform composed of poly(N-isopropylacrylamide-co-Jeffamine® M-1000 acrylamide) (PNJ copolymers [31–33]) as a scaffold for expanding and enriching GSCs in 3D culture. To identify conditions under which the GSC phenotype was enriched, we performed a complete functional characterization (multipotency, self-renewal capacity, and radioresistance) of GSC behaviors alongside analysis of relevant GSC markers. In this study, we utilized two molecularly distinct GSC lines, GB3 (proneural) and GB7 (classical), primarily to illustrate the robustness of effects from the PNJ culture system. Evaluation of subtype-specific responses would be an interesting avenue for future work. In all, we utilized this approach to identify conditions within an engineered *in vitro* 3D microenvironment that positively regulate the GSC phenotype and contribute to radioresistant behaviors.

PNIPAAm is a temperature responsive polymer that exhibits a lower critical solution temperature (LCST) phase transition near 30 °C in aqueous solution [53]. The LCST enables reversible physical crosslinking where the polymer is soluble at room temperature and precipitates to form a non-water soluble scaffold at 37 °C. In the gel state, PNIPAAm scaffolds experience significant phase separation due to hydrophobic chain interactions which limits their utility in 3D culture. The phase separation of PNIPAAm is reduced considerably by copolymerization with Jeffamine M-1000® acrylamide (JAAm) [32], which generates PNJ copolymers that exhibit fast dissolution to enable transient 3D cell culture [33]. In this study, the biochemical properties of PNJ scaffolds were tuned by modulating JAAm incorporation to form the three different PNJ formulations (PNJ10, PNJ15, PNJ20). Increasing JAAm concentration effects a corresponding increase in equilibrium water content in the scaffold [32]. The physical properties of PNJ scaffolds can also be easily tuned by altering the dissolved copolymer concentration. At the concentrations tested, PNJ copolymers formed viscoelastic ($G' > G''$) scaffolds with stiffness (G') ranging from 153 to 1240 Pa (Fig. 1) which directly coincides with the stiffness of healthy brain tissue [54]. We also observed that JAAm content affected PNJ scaffold stiffness, and that this effect was amplified in the higher concentration constructs. Overall, the tunable nature of the PNJ platform enables analysis of cell responses to variations in both microenvironmental chemistry and stiffness. For these studies, we chose to utilize soft scaffolds (153 – 325 Pa) to model the microenvironment. Stable cell culture scaffolds in this stiffness range are currently underreported as they may be difficult to create with chemical crosslinking strategies due to a low incipient density of crosslinks.

One initial observation of PNJ cultured GSCs was that cells did not cluster into large aggregates that are common in standard neurosphere cultures. During gelation, the physically crosslinked scaffolds form a polymeric network that segregates and suspends the cells in their location. Over the course of the culture, the cells grow as individual spheres that do not contact neighboring spheres as they inevitably do during free flotation in culture media. This caused GSCs to grow in significantly smaller and more uniform spheres in PNJ scaffolds compared to neurosphere conditions (Fig. 2). This phenomenon has also been reported in other 3D scaffold systems [29,55]. One of the primary drawbacks of neurosphere culture is that nutrient gradients develop quickly in relation to sphere size and have an adverse effect on stem enrichment [17,18]. To this end, viscoelastic PNJ scaffolds prevent sphere aggregation and thus provide microenvironmental conditions that are fundamentally distinct from neurosphere or large organoid cultures. These conditions may positively contribute to enrichment of the GSC phenotype; it would be interesting, in future work, to consider hanging drop culture or culture within micro-patterned wells as methods to further define and control neurosphere size [56].

We measured functional GSC characteristics of GB3 and GB7 cells cultured in PNJ scaffolds to determine how stem phenotypes may be altered in comparison to neurosphere conditions. GSCs cannot be identified by a single feature but instead require multifaceted characterization. Multipotency, is a direct driver of GBM tumor heterogeneity as GSCs are capable of generating a diverse hierarchy of neoplastic cells that work to support tumor maintenance and growth [4,5,15]. Here, we observed that cells propagated in neurosphere culture as well in PNJ scaffold cultures were capable of multipotent differentiation (Fig. 3) as measured by expression of proteins associated with three neural subtypes (neurons, oligodendrocytes, astrocytes). Importantly, differentiating GSCs will often promiscuously express differentiation markers of multiple neuronal lineages in ways that are not observed in healthy neural stem cells [5,6,15]. Thus, positive staining indicating overlapping expression of these antigens is possible under the described conditions. This phenomenon is generally ascribed to aberrant activation of differentiation machinery as a result of the malignant

transformation that affects these tumor cells.

Self-renewal is another essential GSC characteristic that is a primary driver of tumorigenicity and recurrence *in vivo* [5,7,8]. We assayed the self-renewal capacity of GB3 and GB7 cells using an *in vitro* limiting dilution assay. *In vivo* limiting dilution is one of the gold standard methods for GSC identification but it is not directly quantitative. Given that the control (neurosphere) cultures were previously characterized as containing GSCs [35,36], the *in vitro* limiting dilution and subsequent ELDA analysis were employed to measure quantitative differences in stem cell frequency [8,37]. Using this method, the stem cell frequency of PNJ cultured GB3 and GB7 cells was measured to be significantly increased ($p < 0.01$) for all scaffold formulations compared to neurosphere cultured controls (Fig. 4). To our knowledge, this is the first report of a 3D biomaterial that increases self-renewal capacity in patient-derived GSC cultures. Mebiol® gel scaffolds have been shown to be useful for maintaining multipotent patient-derived GBM cells, but functional stem enrichment was not directly measured [29]. While Mebiol® gel and PNJ are chemically similar, the reported scaffold stiffness (1000 Pa) is more than three times greater than the stiffest PNJ scaffold (325 Pa) and may play a role in this dichotomy. Alternatively, Matrigel® cultured GSCs reportedly develop GBM tumor organoids that reduce self-renewal capacity of the original stem population [30]. In contrast to Matrigel®, which contains both serum and extracellular matrix proteins, synthetic PNJ scaffolds do not provide any bioactive or native niche cues. Yet, the biochemical and biophysical properties of these scaffolds provide permissive conditions for non-adherent neurosphere growth that maintain GSCs in an undifferentiated state and increase self-renewal capacity. The interplay of effects imparted by the biochemical and biophysical properties of the scaffold is an important and likely complex relationship that warrants future study.

PNJ cultures also altered the expression of proteins that are attributed to the GSC phenotype. Specifically, NESTIN and EGFR expression were increased in both cell lines across all scaffold conditions (Fig. 5). NESTIN is an established NSC marker and has been shown to regulate self-renewal capacity [57,58]. The EGFR pathway is one of the most studied in GBM biology as it is frequently amplified and/or mutated in the disease state [59]. Moreover, EGFR signaling in GSCs has been shown to help maintain the molecular characteristics of the original tumor sample [15], and also regulate their self-renewal capacity *in vitro* [60]. Thus, increases in NESTIN and EGFR expression are consistent with the measured increase in GB3 and GB7 self-renewal. Additionally, expression of the hyaluronic acid receptor CD44 was also increased in PNJ cultured GB3 cells as well as PNJ10 and PNJ20 cultured GB7 cells. CD44 expression has been proposed as a GSC marker and is commonly associated with an invasive phenotype [35,39]. Taken together, these data suggest that PNJ scaffolds promote expression of proteins that are known to regulate key GSC phenotypes such as self-renewal and invasion.

In vivo, GSCs are concentrated in specific niches (hypoxic, invasive, and perivascular), each of which may regulate cellular phenotype via distinct mechanisms [13]. Culturing GSCs as neurospheres or organoids is expected to drive cellular evolution primarily as a result of the gradients of oxygen and nutrient deprivation, which develop as cells proliferate [17,18]. In contrast, the PNJ microenvironment is expected to be relatively nutrient and oxygen rich. This expectation is based on the relatively small size of neurospheres grown within the gel (which prevents formation of a necrotic core), as well as our previous work showing that PNJ scaffolds retain encapsulated protein [32]. It is possible that proteins secreted by GSCs in PNJ scaffolds are effectively sequestered near cells, leading to increased autocrine signaling. The increased expression of EGFR we observed in these studies supports this hypothesis, and the small size of clonogenic spheres produced by PNJ cultures draws further parallel to the *in vivo* circumstance, where GSCs are found in small clusters near blood vessels. We thus propose that the PNJ microenvironment may be a relevant model for GSC interactions with the perivascular niche [14,40].

From a clinical perspective, total surgical resection of GBM tumors is often impossible due to tumor location and the potential for damage to healthy brain tissue. As a result, radiation offers the best treatment modality for remaining tumorigenic cells due to its ability to directly penetrate the target tissue. However, radiotherapy is resisted by GSCs that respond with increased activation of DNA damage repair pathways [10]. This behavior, similar to self-renewal capacity, enables GSCs to mediate tumor recurrence and disease progression. Moreover, support from the GSC niche is believed to be significant driver of radioresistance [13,14,40–42]. Hubert et al. investigated this by irradiating GSC derived 3D GBM organoids and found that GSC marker expression was inversely correlated with apoptotic marker expression [30]. In our work, populations of PNJ cultured GSCs displayed significantly increased radioresistance in an experimental model that directly assayed cell viability in response to treatment (Fig. 6). Additionally, EGFR activity has been studied as a driver of GBM radioresistance [61,62] and may in this context be a contributing factor to the behavior we observed. These data suggest that 3D cultures, and specifically PNJ scaffolds, are valuable tools for studying microenvironmental support of radioresistance *in vitro*; we propose that these microenvironments are an effective model for GSC niches that are implicated in driving treatment resistance and tumor recurrence *in vivo* [40].

5. Conclusion

This work describes 3D culture conditions that were implemented using fully synthetic PNJ scaffolds to expand and enrich GSCs in culture. Using these scaffolds, we measured enrichment of functional GSC characteristics, including radioresistance, as well as corresponding protein expression in two molecularly distinct patient-derived models of GBM. The tunable nature of the PNJ platform is a substantial advantage as it enables control over the chemical and physical properties of the scaffold to study niche regulation of GSCs in a variety of conditions. PNJ chemistry also presents the opportunity for additional engineering; for example, by inclusion of bioactive peptides such as RGD to study cell adhesion related GSC-niche interactions [33]. In conclusion, we propose that the PNJ platform offers significant opportunities for studying microenvironmental regulation of clinically relevant models of GBM *in vitro*. Although current methods of GBM treatment have proven minimally effective, future therapeutic strategies may achieve a higher degree of success by focusing on disruption of GSC regulatory mechanisms within the microenvironment.

Acknowledgements

Patient-derived GBM cells were provided by the Biobank Core Facility at St. Joseph's Hospital and Medical Center and Barrow Neurological Institute which is funded by the Arizona Biomedical Research Commission and the Barrow Neurological Foundation. We thank Robert Kupp, Jonathan Yamaguchi, and Emily Szeto for their assistance in establishing and maintaining patient-derived GBM cell lines. We also gratefully acknowledge funding support for this work from the Barrow Neurological Foundation, the Phoenix chapter of the Achievement Rewards for Collegiate Scientists (ARCS) Foundation, the National Institute of Neurological Disorders and Stroke (NINDS, R01 NS088648A), and the Ben and Catherine Ivy Foundation.

References

[1] R. Stupp, M.E. Hegi, W.P. Mason, M.J. van den Bent, M.J. Taphoorn, R.C. Janzer, S.K. Ludwin, A. Allgeier, B. Fisher, K. Belanger, P. Hau, A.A. Brandes, J. Gijtenbeek, C. Marosi, C.J. Vecht, K. Mokhtari, P. Wesseling, S. Villa, E. Eisenhauer, T. Gorlia, M. Weller, D. Lacombe, J.G. Cairncross, R.-O. Mirimanoff, Effects of radiotherapy with concomitant and adjuvant temozolomide versus radiotherapy alone on survival in glioblastoma in a randomised phase III study: 5-year analysis of the EORTC-NCIC trial, Lancet Oncol. 10 (2009) 459–466, http://dx.doi.org/10.1016/S1470-2045(09)70025-7.

[2] A. Omuro, L.M. DeAngelis, Glioblastoma and other malignant gliomas: a clinical review, JAMA 310 (2013) 1842–1850, http://dx.doi.org/10.1001/jama.2013.280319.

[3] M. Venere, H.A. Fine, P.B. Dirks, J.N. Rich, Cancer stem cells in gliomas: identifying and understanding the apex cell in cancer's hierarchy, Glia 59 (2011) 1148–1154, http://dx.doi.org/10.1002/glia.21185.

[4] N. Sanai, A. Alvarez-Buylla, M.S. Berger, Neural stem cells and the origin of gliomas, N. Engl. J. Med. 353 (2005) 811–822, http://dx.doi.org/10.1056/NEJMra043666.

[5] R. Galli, E. Binda, U. Orfanelli, B. Cipelletti, A. Gritti, S.D. Vitis, R. Fiocco, C. Foroni, F. Dimeco, A. Vescovi, Isolation and characterization of tumorigenic, stem-like neural precursors from human glioblastoma, Cancer Res. 64 (2004) 7011–7021, http://dx.doi.org/10.1158/0008-5472.CAN-04-1364.

[6] T.N. Ignatova, V.G. Kukekov, E.D. Laywell, O.N. Suslov, F.D. Vrionis, D.A. Steindler, Human cortical glial tumors contain neural stem-like cells expressing astroglial and neuronal markers in vitro, Glia 39 (2002) 193–206, http://dx.doi.org/10.1002/glia.10094.

[7] S.K. Singh, I.D. Clarke, M. Terasaki, V.E. Bonn, C. Hawkins, J. Squire, P.B. Dirks, Identification of a cancer stem cell in human brain tumors, Cancer Res. 63 (2003) 5821–5828.

[8] S. Singh, C. Hawkins, I. Clarke, J. Squire, J. Bayani, T. Hide, M. Henkelman, M. Cusimano, P. Dirks, Identification of human brain tumour initiating cells, Nature 432 (2004) 393–396, http://dx.doi.org/10.1038/nature03031.

[9] L. Cheng, Q. Wu, O.A. Guryanova, Z. Huang, Q. Huang, J.N. Rich, S. Bao, Elevated invasive potential of glioblastoma stem cells, Biochem. Biophys. Res. Commun. 406 (2011) 643–648, http://dx.doi.org/10.1016/j.bbrc.2011.02.123.

[10] S. Bao, Q. Wu, R.E. McLendon, Y. Hao, Q. Shi, A.B. Hjelmeland, M.W. Dewhirst, D.D. Bigner, J.N. Rich, Glioma stem cells promote radioresistance by preferential activation of the DNA damage response, Nature 444 (2006) 756–760, http://dx.doi.org/10.1038/nature05236.

[11] A. Eramo, L. Ricci-Vitiani, A. Zeuner, R. Pallini, F. Lotti, G. Sette, E. Pilozzi, L.M. Larocca, C. Peschle, R. De Maria, Chemotherapy resistance of glioblastoma stem cells, Cell Death Differ. 13 (2006) 1238–1241, http://dx.doi.org/10.1038/sj.cdd.4401872.

[12] A. Murat, E. Migliavacca, T. Gorlia, W.L. Lambiv, T. Shay, M.-F. Hamou, N. de Tribolet, L. Regli, W. Wick, M.C.M. Kouwenhoven, J.A. Hainfellner, F.L. Heppner, P.-Y. Dietrich, Y. Zimmer, J.G. Cairncross, R.-C. Janzer, E. Domany, M. Delorenzi, R. Stupp, M.E. Hegi, Stem Cell–Related "Self-Renewal" Signature and High Epidermal Growth factor receptor expression associated with resistance to concomitant chemoradiotherapy in glioblastoma, J. Clin. Oncol. 26 (2008) 3015–3024, http://dx.doi.org/10.1200/JCO.2007.15.7164.

[13] J.D. Lathia, J.M. Heddleston, M. Venere, J.N. Rich, Deadly teamwork: neural cancer stem cells and the tumor microenvironment, Cell Stem Cell. 8 (2011) 482–485, http://dx.doi.org/10.1016/j.stem.2011.04.013.

[14] R.J. Gilbertson, J.N. Rich, Making a tumour's bed: glioblastoma stem cells and the vascular niche, Nat. Rev. Cancer 7 (2007) 733–736.

[15] J. Lee, S. Kotliarova, Y. Kotliarov, A. Li, Q. Su, N.M. Donin, S. Pastorino, B.W. Purow, N. Christopher, W. Zhang, J.K. Park, H.A. Fine, Tumor stem cells derived from glioblastomas cultured in bFGF and EGF more closely mirror the phenotype and genotype of primary tumors than do serum-cultured cell lines, Cancer Cell. 9 (2006) 391–403, http://dx.doi.org/10.1016/j.ccr.2006.03.030.

[16] K. Woolard, H.A. Fine, Glioma stem cells: better flat than round, Cell Stem Cell. 4 (2009) 466–467, http://dx.doi.org/10.1016/j.stem.2009.05.013.

[17] A. Bez, E. Corsini, D. Curti, M. Biggiogera, A. Colombo, R.F. Nicosia, S.F. Pagano, E.A. Parati, Neurosphere and neurosphere-forming cells: morphological and ultrastructural characterization, Brain Res. 993 (2003) 18–29, http://dx.doi.org/10.1016/j.brainres.2003.08.061.

[18] D. Beier, J. Wischhusen, W. Dietmaier, P. Hau, M. Proescholdt, A. Brawanski, U. Bogdahn, C.P. Beier, CD133 expression and cancer stem cells predict prognosis in high-grade oligodendroglial tumors, Brain Pathol. 18 (2008) 370–377, http://dx.doi.org/10.1111/j.1750-3639.2008.00130.x.

[19] S.M. Pollard, K. Yoshikawa, I.D. Clarke, D. Danovi, S. Stricker, R. Russell, J. Bayani, R. Head, M. Lee, M. Bernstein, J.A. Squire, A. Smith, P. Dirks, Glioma stem cell lines expanded in adherent culture have tumor-specific phenotypes and are suitable for chemical and genetic screens, Cell Stem Cell. 4 (2009) 568–580, http://dx.doi.org/10.1016/j.stem.2009.03.014.

[20] M.J. Son, K. Woolard, D.-H. Nam, J. Lee, H.A. Fine, SSEA-1 is an enrichment marker for tumor-initiating cells in human glioblastoma, Cell Stem Cell. 4 (2009) 440–452, http://dx.doi.org/10.1016/j.stem.2009.03.003.

[21] J.D. Lathia, J. Gallagher, J.M. Heddleston, J. Wang, C.E. Eyler, J. MacSwords, Q. Wu, A. Vasanji, R.E. McLendon, A.B. Hjelmeland, J.N. Rich, Integrin alpha 6 regulates glioblastoma stem cells, Cell Stem Cell. 6 (2010) 421–432, http://dx.doi.org/10.1016/j.stem.2010.02.018.

[22] C. Venugopal, N.M. McFarlane, S. Nolte, B. Manoranjan, S.K. Singh, Processing of primary brain tumor tissue for stem cell assays and flow sorting, J. Vis. Exp. (2012), http://dx.doi.org/10.3791/4111.

[23] J.D. Lathia, S.C. Mack, E.E. Mulkearns-Hubert, C.L.L. Valentim, J.N. Rich, Cancer stem cells in glioblastoma, Genes Dev. 29 (2015) 1203–1217, http://dx.doi.org/10.1101/gad.261982.115.

[24] S.J. Florczyk, K. Wang, S. Jana, D.L. Wood, S.K. Sytsma, J.G. Sham, F.M. Kievit, M. Zhang, Porous chitosan-hyaluronic acid scaffolds as a mimic of glioblastoma microenvironment ECM, Biomaterials 34 (2013) 10143–10150, http://dx.doi.org/10.1016/j.biomaterials.2013.09.034.

[25] F.M. Kievit, S.J. Florczyk, M.C. Leung, K. Wang, J.D. Wu, J.R. Silber, R.G. Ellenbogen, J.S.H. Lee, M. Zhang, Proliferation and enrichment of CD133+ glioblastoma cancer stem cells on 3D chitosan-alginate scaffolds, Biomaterials 35 (2014) 9137–9143, http://dx.doi.org/10.1016/j.biomaterials.2014.07.037.

[26] F.M. Kievit, K. Wang, A.E. Erickson, S.K. Lan Levengood, R.G. Ellenbogen, M. Zhang, Modeling the tumor microenvironment using chitosan-alginate scaffolds to control the stem-like state of glioblastoma cells, Biomater. Sci. (2016), http://dx.doi.org/10.1039/C5BM00514K.

[27] N.K.L. Ma, J.K. Lim, M.F. Leong, E. Sandanaraj, B.T. Ang, C. Tang, A.C.A. Wan, Collaboration of 3D context and extracellular matrix in the development of glioma stemness in a 3D model, Biomaterials 78 (2016) 62–73, http://dx.doi.org/10.1016/j.biomaterials.2015.11.031.

[28] S. Zhang, R. Xie, F. Wan, F. Ye, D. Guo, T. Lei, Identification of U251 glioma stem cells and their heterogeneous stem-like phenotypes, Oncol. Lett. 6 (2013) 1649–1655, http://dx.doi.org/10.3892/ol.2013.1623.

[29] Q. Li, H. Lin, O. Wang, X. Qiu, S. Kidambi, L.P. Deleyrolle, B.A. Reynolds, Y. Lei, Scalable production of glioblastoma tumor-initiating cells in 3 dimension thermoreversible hydrogels, sci, Rep 6 (2016) 31915, http://dx.doi.org/10.1038/srep31915.

[30] C.G. Hubert, M. Rivera, L.C. Spangler, Q. Wu, S.C. Mack, B.C. Prager, M. Couce, R.E. McLendon, A.E. Sloan, J.N. Rich, A three-dimensional organoid culture system derived from human glioblastomas recapitulates the hypoxic gradients and cancer stem cell heterogeneity of tumors found in vivo, Cancer Res. 76 (2016) 2465–2477, http://dx.doi.org/10.1158/0008-5472.CAN-15-2402.

[31] D.J. Overstreet, R. Huynh, K. Jarbo, R.Y. McLemore, B.L. Vernon, In situ forming, resorbable graft copolymer hydrogels providing controlled drug release, J. Biomed. Mater. Res. A 101A (2013) 1437–1446, http://dx.doi.org/10.1002/jbm.a.34443.

[32] D.J. Overstreet, R.Y. McLemore, B.D. Doan, A. Farag, B.L. Vernon, Temperature-responsive graft copolymer hydrogels for controlled swelling and drug delivery, Soft Mater 11 (2013) 294–304, http://dx.doi.org/10.1080/1539445X.2011.640731.

[33] J.M. Heffernan, D.J. Overstreet, S. Srinivasan, L.D. Le, B.L. Vernon, R.W. Sirianni, Temperature responsive hydrogels enable transient three-dimensional tumor cultures via rapid cell recovery, J. Biomed. Mater. Res. A 104 (2016) 17–25, http://dx.doi.org/10.1002/jbm.a.35534.

[34] K.L. Ligon, J.A. Alberta, A.T. Kho, J. Weiss, M.R. Kwaan, C.L. Nutt, D.N. Louis, C.D. Stiles, D.H. Rowitch, The oligodendroglial lineage marker OLIG2 is universally expressed in diffuse gliomas, J. Neuropathol. Exp. Neurol. 63 (2004) 499–509, http://dx.doi.org/10.1093/jnen/63.5.499.

[35] S.K. Singh, R. Fiorelli, R. Kupp, S. Rajan, E. Szeto, C. Lo Cascio, C.L. Maire, Y. Sun, J.A. Alberta, J.M. Eschbacher, K.L. Ligon, M.E. Berens, N. Sanai, S. Mehta, Post-translational modifications of OLIG2 regulate glioma invasion through the TGF-β pathway, Cell Rep. 16 (2016) 950–966, http://dx.doi.org/10.1016/j.celrep.2016.06.045.

[36] R. Kupp, L. Shtayer, A.-C. Tien, E. Szeto, N. Sanai, D.H. Rowitch, S. Mehta, Lineage-restricted OLIG2-RTK signaling governs the molecular subtype of glioma stem-like cells, Cell Rep. 16 (2016) 2838–2845, http://dx.doi.org/10.1016/j.celrep.2016.08.040.

[37] Y. Hu, G.K. Smyth, ELDA: Extreme limiting dilution analysis for comparing depleted and enriched populations in stem cell and other assays, J. Immunol. Methods 347 (2009) 70–78, http://dx.doi.org/10.1016/j.jim.2009.06.008.

[38] D.L. Schonberg, D. Lubelski, T.E. Miller, J.N. Rich, Brain tumor stem cells: molecular characteristics and their impact on therapy, Mol. Asp. Med. 0 (2014) 82–101, http://dx.doi.org/10.1016/j.mam.2013.06.004.

[39] A. Ariza, D. López, J.L. Mate, M. Isamat, E. Musulen, M. Pujol, A. Ley, J. Navas-palacios, Role of CD44 in the invasiveness of glioblastoma multiforme and the noninvasiveness of meningioma: an immunohistochemistry study, Hum. Pathol. 26 (1995) 1144–1147.

[40] C. Calabrese, H. Poppleton, M. Kocak, T.L. Hogg, C. Fuller, B. Hamner, E.Y. Oh, M.W. Gaber, D. Finklestein, M. Allen, A. Frank, I.T. Bayazitov, S.S. Zakharenko, A. Gajjar, A. Davidoff, R.J. Gilbertson, A perivascular niche for brain tumor stem cells, Cancer Cell. 11 (2007) 69–82, http://dx.doi.org/10.1016/j.ccr.2006.11.020.

[41] S. Bao, Q. Wu, S. Sathornsumetee, Y. Hao, Z. Li, A.B. Hjelmeland, Q. Shi, R.E. McLendon, D.D. Bigner, J.N. Rich, Stem cell–like glioma cells promote tumor angiogenesis through vascular endothelial growth factor, Cancer Res. 66 (2006) 7843–7848, http://dx.doi.org/10.1158/0008-5472.CAN-06-1010.

[42] L. Cheng, Z. Huang, W. Zhou, Q. Wu, S. Donnola, J.K. Liu, X. Fang, A.E. Sloan, Y. Mao, J.D. Lathia, W. Min, R.E. McLendon, J.N. Rich, S. Bao, Glioblastoma stem cells generate vascular pericytes to support vessel function and tumor growth, Cell. 153 (2013) 139–152, http://dx.doi.org/10.1016/j.cell.2013.02.021.

[43] J. Heffernan, D. Overstreet, L. Le, B. Vernon, R. Sirianni, Bioengineered scaffolds for 3D analysis of glioblastoma proliferation and invasion, Ann. Biomed. Eng. (2014) 1–13, http://dx.doi.org/10.1007/s10439-014-1223-1.

[44] B. Ananthanarayanan, Y. Kim, S. Kumar, Elucidating the mechanobiology of

malignant brain tumors using a brain matrix-mimetic hyaluronic acid hydrogel platform, Biomaterials 32 (2011) 7913–7923, http://dx.doi.org/10.1016/j.biomaterials.2011.07.005.
[45] S. Pedron, E. Becka, B.A.C. Harley, Regulation of glioma cell phenotype in 3D matrices by hyaluronic acid, Biomaterials 34 (2013) 7408–7417, http://dx.doi.org/10.1016/j.biomaterials.2013.06.024.
[46] C. Jiguet Jiglaire, N. Baeza-Kallee, E. Denicolaï, D. Barets, P. Metellus, L. Padovani, O. Chinot, D. Figarella-Branger, C. Fernandez, Ex vivo cultures of glioblastoma in three-dimensional hydrogel maintain the original tumor growth behavior and are suitable for preclinical drug and radiation sensitivity screening, Exp. Cell Res. 321 (2014) 99–108, http://dx.doi.org/10.1016/j.yexcr.2013.12.010.
[47] S.Y. Wong, T.A. Ulrich, L.P. Deleyrolle, J.L. MacKay, J.-M.G. Lin, R.T. Martuscello, M.A. Jundi, B.A. Reynolds, S. Kumar, Constitutive activation of myosin-dependent contractility sensitizes glioma tumor-initiating cells to mechanical inputs and reduces tissue invasion, Cancer Res. 75 (2015) 1113–1122, http://dx.doi.org/10.1158/0008-5472.CAN-13-3426.
[48] T.J. Grundy, E. De Leon, K.R. Griffin, B.W. Stringer, B.W. Day, B. Fabry, J. Cooper-White, G.M. O'Neill, Differential response of patient-derived primary glioblastoma cells to environmental stiffness, Sci. Rep. 6 (2016) 23353, http://dx.doi.org/10.1038/srep23353.
[49] J. Cha, S.-G. Kang, P. Kim, Strategies of mesenchymal invasion of patient-derived brain tumors: microenvironmental adaptation, sci. Rep 6 (2016), http://dx.doi.org/10.1038/srep24912.
[50] P. Ruiz-Ontañon, J.L. Orgaz, B. Aldaz, A. Elosegui-Artola, J. Martino, M.T. Berciano, J.A. Montero, L. Grande, L. Nogueira, S. Diaz-Moralli, A. Esparís-Ogando, A. Vazquez-Barquero, M. Lafarga, A. Pandiella, M. Cascante, V. Segura, J.A. Martinez-Climent, V. Sanz-Moreno, J.L. Fernandez-Luna, Cellular Plasticity Confers Migratory, Invasive, Advantages to a population of glioblastoma-initiating cells that infiltrate peritumoral tissue, Stem Cells 31 (2013) 1075–1085, http://dx.doi.org/10.1002/stem.1349.
[51] M. Herrera-Perez, S.L. Voytik-Harbin, J.L. Rickus, Extracellular matrix properties regulate the migratory response of glioblastoma stem cells in three-dimensional culture, Tissue eng. Part A 21 (2015) 2572–2582, http://dx.doi.org/10.1089/ten.tea.2014.0504.
[52] G. Fernandez-Fuente, P. Mollinedo, L. Grande, A. Vazquez-Barquero, J.L. Fernandez-Luna, Culture dimensionality influences the resistance of glioblastoma stem-like cells to multikinase inhibitors, mol, Cancer Ther. 13 (2014) 1664–1672, http://dx.doi.org/10.1158/1535-7163.MCT-13-0854.
[53] H.G. Schild, Poly (N-isopropylacrylamide): experiment, theory and application, Prog. Polym. Sci. 17 (1992) 163–249.
[54] P.C. Georges, W.J. Miller, D.F. Meaney, E.S. Sawyer, P.A. Janmey, Matrices with compliance comparable to that of brain tissue select neuronal over glial growth in mixed cortical cultures, Biophys. J. 90 (2006) 3012–3018, http://dx.doi.org/10.1529/biophysj.105.073114.
[55] Y. Oh, J. Cha, S.-G. Kang, P. Kim, A polyethylene glycol-based hydrogel as macroporous scaffold for tumorsphere formation of glioblastoma multiforme, J. Ind. Eng. Chem. (2016), http://dx.doi.org/10.1016/j.jiec.2016.05.012.
[56] A. Higuchi, Q.-D. Ling, S. Suresh Kumar, Y. Chang, A.A. Alarfaj, M.A. Munusamy, K. Murugan, S.-T. Hsu, A. Umezawa, Physical cues of cell culture materials lead the direction of differentiation lineages of pluripotent stem cells, J. Mater. Chem. B 3 (2015) 8032–8058, http://dx.doi.org/10.1039/C5TB01276G.
[57] A. Kawaguchi, T. Miyata, K. Sawamoto, N. Takashita, A. Murayama, W. Akamatsu, M. Ogawa, M. Okabe, Y. Tano, S.A. Goldman, H. Okano, Nestin-egfp transgenic mice: visualization of the self-renewal and multipotency of CNS stem cells, Mol. Cell. Neurosci. 17 (2001) 259–273, http://dx.doi.org/10.1006/mcne.2000.0925.
[58] D. Park, A.P. Xiang, F.F. Mao, L. Zhang, C.-G. Di, X.-M. Liu, Y. Shao, B.-F. Ma, J.-H. Lee, K.-S. Ha, N. Walton, B.T. Lahn, Nestin is required for the proper self-renewal of neural stem cells, Stem Cells 28 (2010) 2162–2171, http://dx.doi.org/10.1002/stem.541.
[59] R.G.W. Verhaak, K.A. Hoadley, E. Purdom, V. Wang, Y. Qi, M.D. Wilkerson, C.R. Miller, L. Ding, T. Golub, J.P. Mesirov, G. Alexe, M. Lawrence, M. O'Kelly, P. Tamayo, B.A. Weir, S. Gabriel, W. Winckler, S. Gupta, L. Jakkula, H.S. Feiler, J.G. Hodgson, C.D. James, J.N. Sarkaria, C. Brennan, A. Kahn, P.T. Spellman, R.K. Wilson, T.P. Speed, J.W. Gray, M. Meyerson, G. Getz, C.M. Perou, D.N. Hayes, Integrated genomic analysis identifies clinically relevant subtypes of glioblastoma characterized by abnormalities in PDGFRA, IDH1, EGFR, and NF1, Cancer Cell. 17 (2010) 98–110, http://dx.doi.org/10.1016/j.ccr.2009.12.020.
[60] A. Soeda, A. Inagaki, N. Oka, Y. Ikegame, H. Aoki, S. Yoshimura, S. Nakashima, T. Kunisada, T. Iwama, Epidermal growth factor plays a crucial role in mitogenic regulation of human brain tumor stem cells, J. Biol. Chem. 283 (2008) 10958–10966, http://dx.doi.org/10.1074/jbc.M704205200.
[61] A. Chakravarti, A. Chakladar, M.A. Delaney, D.E. Latham, J.S. Loeffler, The epidermal growth factor receptor pathway mediates resistance to sequential administration of radiation and chemotherapy in primary human glioblastoma cells in a RAS-dependent manner, Cancer Res. 62 (2002) 4307–4315.
[62] J.N. Sarkaria, B.L. Carlson, M.A. Schroeder, P. Grogan, P.D. Brown, C. Giannini, K.V. Ballman, G.J. Kitange, A. Guha, A. Pandita, C.D. James, Use of an orthotopic xenograft model for assessing the effect of epidermal growth factor receptor amplification on glioblastoma radiation response, Am. Assoc. Cancer Res. 12 (2006) 2264–2271, http://dx.doi.org/10.1158/1078-0432.CCR-05-2510.